JOURNAL OF SOLID STATE CHEMISTRY 53, 13–21 (1984)

# Structural Chemistry of Magnéli Phases $Ti_nO_{2n-1}$ ($4 \leq n \leq 9$)

## IV. Superstructure in $Ti_4O_7$ at 140 K*

Y. LE PAGE

*Solid State Chemistry, National Research Council, Ottawa, Canada, K1A OR9*

AND M. MAREZIO

*Laboratoire de Cristallographie, Centre National de la Recherche Scientifique, 166 X- 38042 Grenoble Cedex, France*

Received April 25, 1983; in revised form September 26, 1983

The structure of $Ti_4O_7$ was reexamined at 298, 140, and 115 K. The room-temperature and the 115 K structures are essentially as previously reported. Two new observations were made: a considerable cell-parameter change at the lower transition with a 0.3% increase in cell volume on cooling and the existence of a fivefold superstructure at 140 K only. The 140 K phase with cell parameters $a$ = 6.918(1), $b$ = 11.142(2), $c$ = 15.127(3) $\alpha$ = 90.64(1), $\beta$ = 92.79(1), $\gamma$ = 91.45(1) in space group $P\bar{1}$ corresponds to long-range order of the Ti valences. It shows alternate $Ti^{3+}$ and $Ti^{4+}$ slabs parallel to (1 0 $\bar{2}$) and a few valences with intermediate values at the contact between the slabs with the overall appearance of a modulated structure. Pairing of $Ti^{3+}$ ions is observed. Similar to $Ti_6O_{11}$, expansion and contraction of the Ti–Ti distances in the rutile-like chains is correlated with the electrostatic repulsion of the Ti ions so that the $3^+$ slabs are on the whole contracted along $c_{rutile}$ while the $4^+$ slabs are expanded. The previous interpretation of the 140 K phase as a "liquid of bipolarons" should therefore be revised.

## Introduction

The low temperature behavior of the homologous compounds $Ti_4O_7$ and $Ti_6O_{11}$ are strikingly similar, with two transitions each at comparable temperatures (*1*). The structure of $Ti_4O_7$ was studied at 298, 140, and 120 K and the Ti valences were interpreted to be disordered at 298 K, short-range ordered at 140 K, and ordered at the lowest temperature (*2*) with pairing of $Ti^{3+}$ ions. Comparison of structural, magnetic and ESR results led to interpret the intermediate temperature phase as a "liquid of bipolarons" (*3*). A structural study of $Ti_6O_{11}$ at 298, 130, and 115 K (*4–6*) found disordered Ti valences at room-temperature and nearly complete order in two different superstructures at the other temperatures. These recent results prompted us to verify the reported absence of superstructures in $Ti_4O_7$, $Ti_5O_9$, as well as in the corresponding vanadium oxides. This paper reports the structural studies on pure $Ti_4O_7$ single crystals.

## Experimental

The experimental technique follows closely that of (*5*). The index RT indicates

* Issued as NRCC 23107.



0022-4596/84 $3.00

the room-temperature cell of (*7*). Oscillation patterns about $[100]_{RT}$, $[010]_{RT}$, and $[1\bar{1}1]_{RT}$ were performed at 115, 140, and 298 K with graphite-monochromatized Mo$K\alpha$. At 140 K only, extra layers of reflections could be seen, indicating the presence of a superstructure with fivefold multiplication of the primitive unit cell volume. Diffractometer examination of the reflections showed the cell based on the reciprocal vectors $[(\mathbf{a}^* - 2\mathbf{b}^* + \mathbf{c}^*)/5, (\mathbf{a}^* - \mathbf{b}^*), (\mathbf{a}^* + \mathbf{b}^*)]_{RT}$ to be primitive. The corresponding primitive reduced direct cell at intermediate temperature (IT) has the unit vectors $[\mathbf{a}, \mathbf{b}, \mathbf{c}]_{IT} = [(-3\mathbf{a} - \mathbf{b} + \mathbf{c})/2, (-2\mathbf{a} - \mathbf{b}), (-\mathbf{a} - 5\mathbf{b} + \mathbf{c})/2]_{RT}$. This cell is used throughout the structural study of the 140 K phase. The intensity measurement technique is the same as in (*5*). The specifics of the present data collection are listed in Table I together with the cell parameters obtained by least-squares refinement of about 20 intense single-crystal reflections with $2\theta$ around 115°. The large number of unobserved reflections stems from the peculiar intensity modulation that can be seen on the $[100]_{RT} = [\bar{1}21]_{IT}$ oscillation pattern and on the structure factor table: while reflections for which the sum $[h + 2k - l]_{IT}$ is $5n$ are substructure reflections, the reflections for which it is $5n \pm 1$ are fairly strong superstructure reflections, and those for which it is $5n \pm 2$ are systematically weak with a large proportion of unobserved intensities.

TABLE I

DATA COLLECTION PARAMETERS

| | 298 K | 140 K | | 115 K |
|---|---|---|---|---|
| | | Cell | Subcell | |
| $a$ (Å) | 5.597(1) | 6.918(1) | 5.597(1) | 5.626(1) |
| $b$ (Å) | 7.125(1) | 11.142(2) | 7.132(1) | 7.202(1) |
| $c$ (Å) | 20.429(5) | 15.127(3) | 20.364(5) | 20.260(4) |
| $\alpha$ (°) | 67.70(1) | 90.64(1) | 67.76(1) | 67.90(1) |
| $\beta$ (°) | 57.16(1) | 92.79(1) | 57.44(1) | 57.69(1) |
| $\gamma$ (°) | 108.76(1) | 91.45(1) | 109.02(1) | 109.68(1) |
| $V$ (Å$^3$) | 465.25 | 1164.15 | 465.64 | 467.20 |
| Space group | $I\bar{1}$ | $P\bar{1}$ | $I\bar{1}$ | $I\bar{1}$ |
| Subcell-to-cell transformation | | $\begin{vmatrix} -\frac{3}{2} & -\frac{1}{2} & \frac{1}{2} \\ -2 & -1 & 0 \\ -\frac{1}{2} & -\frac{5}{2} & \frac{1}{2} \end{vmatrix}$ | | |
| Radiation | Mo$K\alpha$ | Mo$K\alpha$ | | Mo$K\alpha$ |
| $2\theta$ range (°) | 80 | 50 | | 80 |
| Total number of measurements | 3146 | 4112 | | 3211 |
| Reflections | | | | |
| Independent | 2896 | 4112 | | 2910 |
| Observed | 2064 | 2220 | | 2649 |
| Unobserved | 832 | 1892 | | 261 |
| Crystal shape | Broken with faces, max dimension 0.2 mm | | | |
| Absorption correction | Gaussian | Gaussian | | Gaussian |
| $\langle \Delta I \rangle / \langle I \rangle$ | 0.010 | — | | 0.011 |
| $R_{Fobs}$ | 0.024 | 0.044 | | 0.021 |
| $wR_{Fobs}$ | 0.033 | 0.036 | | 0.026 |
| Parameter | 101 | 222 | | 101 |

Such an intensity distribution is reminiscent of the satellite reflections observed in "modulated structures" (*8*) but the present case is truly a fivefold superstructure with sharp reflections.

## Origin and Nomenclature

The row along $\mathbf{b}_{RT}$ is $[2\bar{1}\bar{2}]_{IT}$ with a period of 5 $\mathbf{b}_{RT}$. This is similar to $Ti_6O_{11}$ at 130 K where the period along $\mathbf{b}_{RT}$ was tripled in a threefold superstructure. Three and five being both odd numbers, the reasoning in (*5*) about origin selection applies here and the middle of a segment of type 1 can be selected to be the origin. The choice of the motif and the nomenclature as shown on Fig. 1 also follows (*5*). The three indices attached to each atom, respectively, correspond to an arbitrary numbering of the atoms in the rutile cell, the number of $\mathbf{c}_{rutile}$ and $\mathbf{b}_{RT}$ translations applied to it.

## Structure Solution and Refinement of the 140 K Phase

The structure solution method applied here is justified in (*5*). The substructure reflections with $h + 2k - l = 5n$ and the superstructure reflections were rescaled separately so that $\langle E^2 \rangle$ was 1.0 for both families of reflections. From the input of 20 known substructure phases, the MULTAN program (*9*) proposed a set of phases which corresponded to a distortion of the Ti array that was used to initiate the block-diagonal least-squares refinement with counting statistics weights. The above mentioned modulation of the superstructure intensities provoked refinement problems (unacceptably low and high thermal parameters) if observed reflections only were used. These problems vanished when all measurements were included and refined with unit weights. The final cycles were with full matrix and isotropic thermal motion. The final

TABLE IIa

ATOMIC PARAMETERS *X*, *Y*, *Z* AND BEQ AT 298 K

| | X | Y | Z | BEQ |
|---|---|---|---|---|
| TI 11 | 0.02005(14) | 0.02026(10) | 0.06617( 4) | 0.46( 3) |
| TI 12 | 0.08430(14) | 0.03970(10) | 0.20133( 4) | 0.48( 3) |
| TI 21 | 0.02777(14) | 0.52717(10) | 0.06279( 4) | 0.47( 3) |
| TI 22 | 0.07998(14) | 0.53775(10) | 0.20114( 4) | 0.45( 3) |
| O 11 | 0.9119 ( 6) | 0.6607 ( 4) | 0.13898(15) | 0.51(14) |
| O 20 | 0.0623 ( 6) | 0.3324 ( 4) | 0.01525(16) | 0.59(15) |
| O 21 | 0.0341 ( 6) | 0.3165 ( 4) | 0.16423(15) | 0.47(14) |
| O 31 | 0.6115 ( 6) | 0.8335 ( 4) | 0.08140(16) | 0.62(14) |
| O 32 | 0.6238 ( 6) | 0.8428 ( 4) | 0.22382(15) | 0.51(15) |
| O 40 | 0.4138 ( 6) | 0.1768 ( 4) | 0.05780(16) | 0.62(15) |
| O 41 | 0.4423 ( 6) | 0.1729 ( 4) | 0.19843(15) | 0.55(15) |

TABLE OF U(I,J) OR U VALUES *100.

| | U11(U) | U22 | U33 | U12 | U13 | U23 |
|---|---|---|---|---|---|---|
| TI 11 | 0.605(18) | 0.592(19) | 0.587(17) | 0.418(16) | -0.466(16) | -0.395(16) |
| TI 12 | 0.592(18) | 0.586(19) | 0.667(17) | 0.415(16) | -0.482(16) | -0.421(16) |
| TI 21 | 0.607(18) | 0.600(19) | 0.569(17) | 0.412(17) | -0.452(16) | -0.385(17) |
| TI 22 | 0.507(17) | 0.532(18) | 0.601(17) | 0.343(16) | -0.408(16) | -0.374(16) |
| O 11 | 0.73 ( 8) | 0.63 ( 8) | 0.66 ( 7) | 0.47 ( 7) | -0.55 ( 7) | -0.46 ( 7) |
| O 20 | 0.97 ( 8) | 0.75 ( 8) | 0.88 ( 8) | 0.65 ( 7) | -0.77 ( 7) | -0.60 ( 7) |
| O 21 | 0.61 ( 8) | 0.58 ( 7) | 0.61 ( 7) | 0.41 ( 7) | -0.49 ( 7) | -0.38 ( 7) |
| O 31 | 0.59 ( 8) | 0.80 ( 8) | 0.69 ( 7) | 0.39 ( 7) | -0.46 ( 7) | -0.47 ( 7) |
| O 32 | 0.62 ( 8) | 0.62 ( 8) | 0.59 ( 7) | 0.40 ( 7) | -0.46 ( 7) | -0.39 ( 7) |
| O 40 | 0.60 ( 8) | 0.81 ( 8) | 0.74 ( 7) | 0.40 ( 7) | -0.52 ( 7) | -0.48 ( 7) |
| O 41 | 0.60 ( 8) | 0.65 ( 8) | 0.65 ( 7) | 0.37 ( 7) | -0.48 ( 7) | -0.38 ( 7) |

*Note.* BEQ is the arithmetic mean of the principal axes of the thermal ellipsoid. Estimated standard deviations refer to the last digit printed.

TABLE IIb

ATOMIC PARAMETERS $X$, $Y$, $Z$ AND BEQ AT 140 K

| | X | Y | Z | BEQ |
|---|---|---|---|---|
| TI110 | 0.13374(18) | 0.89397(11) | 0.00613(8) | 0.095(24) |
| TI120 | 0.36482(19) | 0.68023(12) | 0.03975(9) | 0.36 ( 3) |
| TI210 | 0.32087(18) | 0.80133(11) | 0.80420(8) | 0.102(25) |
| TI220 | 0.42806(19) | 0.42227(11) | 0.15872(8) | 0.23 ( 3) |
| TI111 | 0.47681(19) | 0.30061(12) | 0.39128(9) | 0.33 ( 3) |
| TI121 | 0.24394(18) | 0.52828(12) | 0.35849(8) | 0.24 ( 3) |
| TI211 | 0.27468(18) | 0.41056(11) | 0.58989(8) | 0.135(24) |
| TI221 | 0.04298(19) | 0.62298(12) | 0.56013(9) | 0.41 ( 3) |
| TI112 | 0.07976(19) | 0.50910(12) | 0.78935(9) | 0.39 ( 3) |
| TI122 | 0.15914(18) | 0.28302(12) | 0.23984(8) | 0.25 ( 3) |
| TI212 | 0.11846(19) | 0.39132(12) | 0.00537(9) | 0.46 ( 3) |
| TI222 | 0.35442(19) | 0.18370(12) | 0.03737(8) | 0.26 ( 3) |
| TI113 | 0.32217(18) | 0.29914(12) | 0.80415(9) | 0.29 ( 3) |
| TI123 | 0.43731(18) | 0.92956(11) | 0.15950(8) | 0.17 ( 3) |
| TI213 | 0.51662(18) | 0.19888(12) | 0.60592(9) | 0.28 ( 3) |
| TI223 | 0.22914(18) | 0.02455(11) | 0.35805(8) | 0.20 ( 3) |
| TI114 | 0.27945(18) | 0.90733(11) | 0.59004(8) | 0.213(25) |
| TI124 | 0.04657(19) | 0.12182(12) | 0.56003(9) | 0.41 ( 3) |
| TI214 | 0.07451(19) | 0.00762(12) | 0.79180(9) | 0.31 ( 3) |
| TI224 | 0.15333(19) | 0.78145(11) | 0.23699(8) | 0.26 ( 3) |
| O 110 | 0.3285 ( 7) | 0.3139 ( 4) | 0.9441 (3) | 0.49 ( 8) |
| O 200 | 0.1613 ( 7) | 0.8871 ( 4) | 0.8849 (3) | 0.52 ( 8) |
| O 210 | 0.4254 ( 7) | 0.6960 ( 4) | 0.9118 (3) | 0.35 ( 8) |
| O 310 | 0.3617 ( 7) | 0.4752 ( 5) | 0.8059 (3) | 0.63 ( 8) |
| O 320 | 0.6059 ( 7) | 0.2708 ( 4) | 0.8345 (3) | 0.34 ( 8) |
| O 400 | 0.0911 ( 8) | 0.7214 ( 5) | 0.0217 (3) | 0.72 ( 9) |
| O 410 | 0.3356 ( 7) | 0.5083 ( 5) | 0.0585 (3) | 0.69 ( 8) |
| O 111 | 0.7291 ( 7) | 0.1089 ( 5) | 0.5461 (3) | 0.55 ( 8) |
| O 201 | 0.5390 ( 8) | 0.6877 ( 5) | 0.4832 (3) | 0.81 ( 9) |
| O 211 | 0.8188 ( 7) | 0.4923 ( 4) | 0.5173 (3) | 0.42 ( 8) |
| O 311 | 0.7578 ( 8) | 0.2761 ( 5) | 0.4029 (4) | 0.87 ( 9) |
| O 321 | 0.0126 ( 7) | 0.0704 ( 4) | 0.4326 (3) | 0.53 ( 8) |
| O 401 | 0.4980 ( 8) | 0.5178 ( 5) | 0.6246 (3) | 0.67 ( 8) |
| O 411 | 0.7384 ( 8) | 0.3130 ( 5) | 0.6582 (3) | 0.71 ( 8) |
| O 112 | 0.1430 ( 7) | 0.9111 ( 4) | 0.1419 (3) | 0.42 ( 8) |
| O 202 | 0.9498 ( 7) | 0.4896 ( 5) | 0.0804 (3) | 0.60 ( 8) |
| O 212 | 0.2079 ( 7) | 0.2968 ( 4) | 0.1139 (3) | 0.45 ( 8) |
| O 312 | 0.1459 ( 7) | 0.0735 ( 4) | 0.0031 (3) | 0.30 ( 8) |
| O 322 | 0.4149 ( 7) | 0.8743 ( 5) | 0.0325 (3) | 0.49 ( 8) |
| O 402 | 0.8781 ( 7) | 0.3144 ( 5) | 0.2224 (3) | 0.59 ( 8) |
| O 412 | 0.1317 ( 7) | 0.1078 ( 4) | 0.2591 (3) | 0.39 ( 8) |
| O 113 | 0.5288 ( 7) | 0.7119 ( 5) | 0.7472 (3) | 0.52 ( 8) |
| O 203 | 0.3538 ( 7) | 0.2870 ( 5) | 0.6858 (3) | 0.54 ( 8) |
| O 213 | 0.6228 ( 7) | 0.0922 ( 5) | 0.7141 (3) | 0.62 ( 8) |
| O 313 | 0.5688 ( 7) | 0.8757 ( 4) | 0.6057 (3) | 0.25 ( 8) |
| O 323 | 0.8152 ( 7) | 0.6674 ( 5) | 0.6349 (3) | 0.46 ( 8) |
| O 403 | 0.3057 ( 7) | 0.1212 ( 4) | 0.8238 (3) | 0.19 ( 8) |
| O 413 | 0.5459 ( 7) | 0.9142 ( 4) | 0.8582 (3) | 0.21 ( 8) |
| O 114 | 0.9426 ( 7) | 0.5072 ( 4) | 0.3444 (3) | 0.36 ( 8) |
| O 204 | 0.7363 ( 7) | 0.0850 ( 4) | 0.2825 (3) | 0.26 ( 8) |
| O 214 | 0.0098 ( 7) | 0.8920 ( 5) | 0.3153 (3) | 0.56 ( 8) |
| O 314 | 0.9461 ( 7) | 0.6751 ( 5) | 0.2018 (3) | 0.63 ( 8) |
| O 324 | 0.2167 ( 7) | 0.4740 ( 4) | 0.2313 (3) | 0.37 ( 8) |
| O 404 | 0.6813 ( 7) | 0.9138 ( 5) | 0.4231 (3) | 0.53 ( 8) |
| O 414 | 0.9324 ( 7) | 0.7073 ( 5) | 0.4601 (3) | 0.52 ( 8) |

*Note.* BEQ was calculated as $8\pi^2\bar{u}^2$ where $\bar{u}^2$ is the refined mean square thermal displacement.

residuals were $R_F = 0.096$ on all measurements $R_F = 0.044$, $wR_F = 0.036$ on the 2220 observed ones. The weighted residual quoted was calculated with counting statistics weights after unit weight refinement.

The refinements of the structures at 298 and 115 K were performed by means of full matrix least-squares with counting statistics weights and anisotropic thermal motion. The final residuals are $R_F = 0.024$ and $wR_F = 0.033$ at 298 K and $R_F = 0.021$, $wR_F = 0.026$ at 115 K. The final atomic positions

TABLE IIc

ATOMIC PARAMETERS *X*, *Y*, *Z* AND BEQ AT 115 K

| | X | Y | Z | BEQ |
|---|---|---|---|---|
| TI 11 | 0.01623(8) | 0.04010(6) | 0.065651(23) | 0.251(20) |
| TI 12 | 0.09261(9) | 0.04084(6) | 0.204340(23) | 0.242(21) |
| TI 21 | 0.03165(8) | 0.52671(6) | 0.068268(22) | 0.246(20) |
| TI 22 | 0.08833(8) | 0.55111(6) | 0.193794(23) | 0.240(21) |
| O 11 | 0.8895 (4) | 0.6604 (3) | 0.14219 (10) | 0.33 ( 9) |
| O 20 | 0.0583 (4) | 0.3288 (3) | 0.01655 (10) | 0.37 ( 9) |
| O 21 | 0.0221 (4) | 0.2993 (3) | 0.16871 (10) | 0.32 ( 9) |
| O 31 | 0.6336 (4) | 0.8480 (3) | 0.07434 (10) | 0.34 ( 9) |
| O 32 | 0.6171 (4) | 0.8346 (3) | 0.22258 (10) | 0.33 ( 9) |
| O 40 | 0.3938 (4) | 0.1728 (3) | 0.06198 (10) | 0.35 ( 9) |
| O 41 | 0.4435 (4) | 0.1748 (3) | 0.19785 (10) | 0.37 (10) |

TABLE OF U(I, J) OR U VALUES *100.

| | U11(U) | U22 | U33 | U12 | U13 | U23 |
|---|---|---|---|---|---|---|
| TI 11 | 0.359(11) | 0.334(11) | 0.312(10) | 0.253(10) | -0.266(10) | -0.223(9) |
| TI 12 | 0.318(11) | 0.336(10) | 0.314(10) | 0.241(10) | -0.252( 9) | -0.219(9) |
| TI 21 | 0.321(11) | 0.320(11) | 0.272(10) | 0.233(10) | -0.219(10) | -0.192(9) |
| TI 22 | 0.272(11) | 0.309(10) | 0.300(10) | 0.206(10) | -0.214( 9) | -0.198(9) |
| O 11 | 0.44 ( 5) | 0.44 ( 5) | 0.39 ( 4) | 0.31 ( 4) | -0.31 ( 4) | -0.27 (4) |
| O 20 | 0.62 ( 5) | 0.49 ( 5) | 0.54 ( 5) | 0.43 ( 4) | -0.48 ( 4) | -0.38 (4) |
| O 21 | 0.43 ( 5) | 0.39 ( 5) | 0.45 ( 4) | 0.30 ( 4) | -0.34 ( 4) | -0.28 (4) |
| O 31 | 0.35 ( 5) | 0.47 ( 5) | 0.41 ( 4) | 0.25 ( 4) | -0.30 ( 4) | -0.30 (4) |
| O 32 | 0.41 ( 5) | 0.39 ( 5) | 0.38 ( 4) | 0.27 ( 4) | -0.29 ( 4) | -0.26 (4) |
| O 40 | 0.36 ( 5) | 0.48 ( 5) | 0.40 ( 4) | 0.27 ( 4) | -0.29 ( 4) | -0.29 (4) |
| O 41 | 0.43 ( 5) | 0.47 ( 5) | 0.45 ( 4) | 0.30 ( 4) | -0.35 ( 4) | -0.29 (4) |

*Note.* BEQ is the arithmetic mean of the principal axes of the thermal ellipsoid. Estimated standard deviations refer to the last digit printed.

are listed in Table II together with equivalent isotropic thermal motion.[1] Table III gives the Ti valences as derived from the Ti–O distances using bond-valence summation with the bond length–bond strength relationship from (*11*) applied as in (*5*).

## Discussion

The observation of the fivefold superstructure clearly establishes the existence of a long-range charge localization.

[1] See NAPS document No. 04168 for 66 pages of supplementary material. Order from ASIS/NAPS, Microfiche Publications, P.O. Box 3513, Grand Central Station, New York, NY 10163. Remit in advance $4.00 for microfiche copy or for photocopy, $7.75 up to 20 pages plus $.30 for each additional page. All orders must be prepaid. Institutions and organizations may order by purchase order. However, there is a billing and handling charge for this service of $15. Foreign orders add $4.50 for postage and handling, for the first 20 pages, and $1.00 for additional 10 pages of material. Remit $1.50 for postage of any microfiche orders.

The superstructure reflections are so weak that the background reduction of monochromatic versus filtered radiation might be essential to the photographic observation of the reflections and may explain why they were overlooked in $Ti_4O_7$ (*2*) and $Ti_5O_9$ (*10*) in spite of the fact that such a possibility was investigated. It is also possible that, due to the different transport agents and growth rates used in the preparation of the crystals ($Cl_2$ vs $TeCl_4$), the long-range order which gives in the present investigation sharp diffraction spots might correspond to shorter-range order in other samples giving wider, less dense photographic spots that would be more difficult to see.

Table IV shows the cell data from (*2*) and (*14*), respectively, for pure and V-doped $Ti_4O_7$ together with the results on the present sample. Although the sample used here was not analyzed, it comes from a series of similar preparations (15) where the

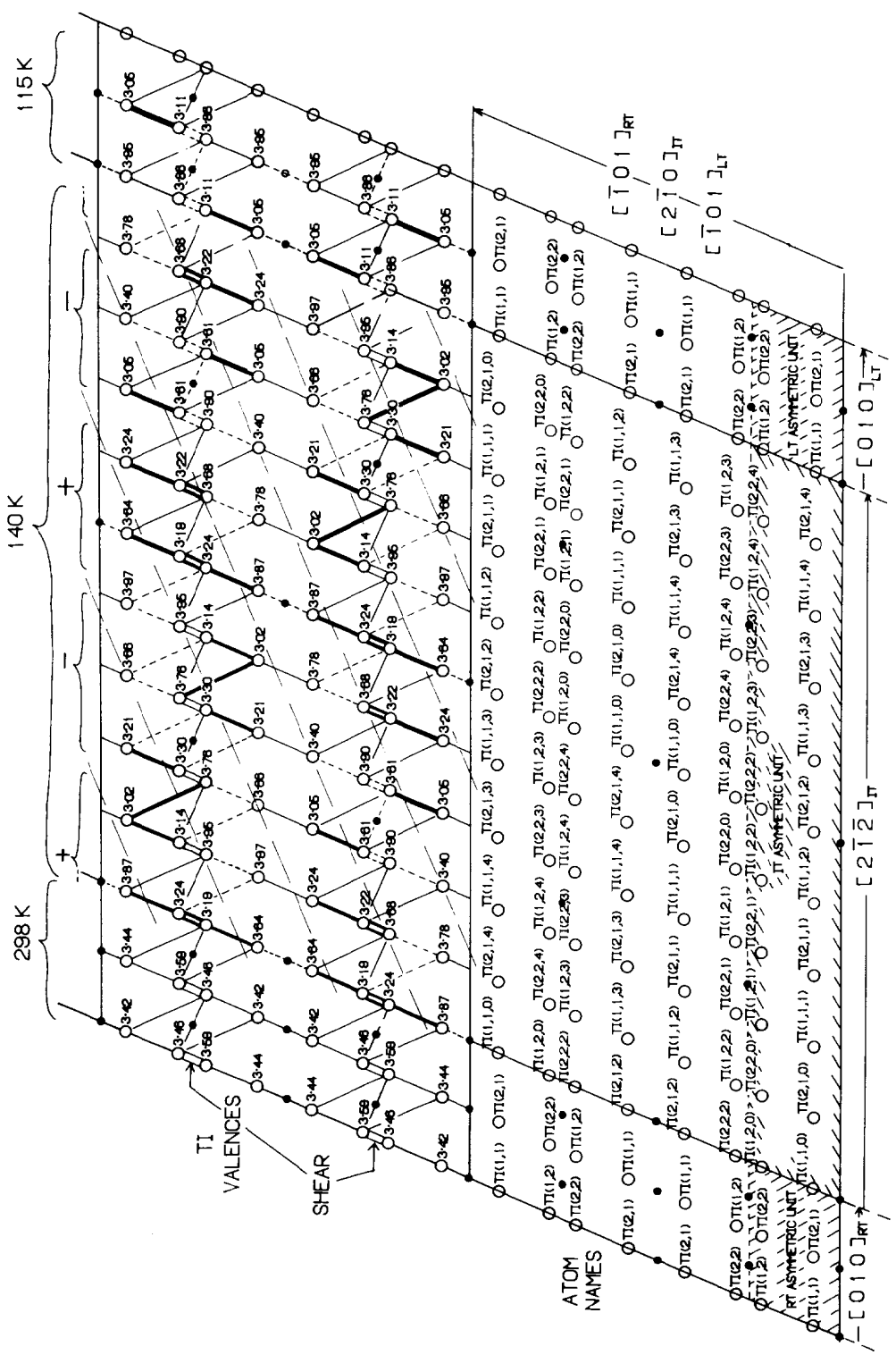


FIG. 1. Projection along $a_{RT}$ of a $(101)_{RT}$ slab of edge- and face-sharing $TiO_6$ octahedra for the three phases studied. The origin is at the lower left corner in the three cases. For a representation of the octahedra themselves see Ref. (*7*). The Ti valences shown were obtained by bond-valence summation (*11*) on the observed Ti–O distances. Single lines between the Ti atoms symbolize edge-sharing, double lines the face-sharing in the shear plane. Thick lines indicate a shortening of the corresponding Ti–Ti distance by more than 0.05 Å with respect to the RT phase, dotted lines a similar lengthening. The oblique dotted lines at IT limit the slabs designed by (+) and (−) where the Ti valences are respectively seen to increase and decrease with respect to the RT distribution. ●, Inversion centers.

TABLE III

Ti–Ti Distances

| 298 K | | 140 K | | 115 K | |
|---|---|---|---|---|---|
| | | In the $[10]_{RT}$ chains | | | |
| Ti(1,1)–Ti(1,1) 2.941 | Ti(1,1,0)–Ti(1,1,0) 3.040 | Ti(1,1,1)–Ti(1,1,4) 2.908 | Ti(1,1,2)–Ti(1,1,3) 2.917 | Ti(1,1,3)–Ti(1,1,2) 2.917 | Ti(1,1,4)–Ti(1,1,1) 2.908 | Ti(1,1)–Ti(1,1) 3.008 |
| Ti(1,1)–Ti(1,2) 3.018 | Ti(1,1,0)–Ti(1,2,0) 2.937 | Ti(1,1,1)–Ti(1,2,1) 3.071 | Ti(1,1,2)–Ti(1,2,2) 2.905 | Ti(1,1,3)–Ti(1,2,3) 3.118 | Ti(1,1,4)–Ti(1,2,4) 2.943 | Ti(1,1)–Ti(1,2) 3.063 |
| Ti(1,2)–Ti(2,2) 2.812 | Ti(1,2,0)–Ti(2,2,2) 2.746 | Ti(1,2,1)–Ti(2,2,1) 2.900 | Ti(1,2,2)–Ti(2,2,0) 2.737 | Ti(1,2,3)–Ti(2,2,4) 2.839 | Ti(1,2,4)–Ti(2,2,3) 2.820 | Ti(1,2)–Ti(2,2) 2.861 |
| Ti(2,1)–Ti(2,1) 2.893 | Ti(2,1,0)–Ti(2,1,4) 2.898 | Ti(2,1,1)–Ti(2,1,3) 2.932 | Ti(2,1,2)–Ti(2,1,2) 2.960 | Ti(2,1,3)–Ti(2,1,1) 2.932 | Ti(2,1,4)–Ti(2,1,0) 2.898 | Ti(2,1)–Ti(2,1) 3.113 |
| Ti(2,1)–Ti(2,2) 3.020 | Ti(2,1,0)–Ti(2,2,0) 3.114 | Ti(2,1,1)–Ti(2,2,1) 2.919 | Ti(2,1,2)–Ti(2,2,2) 2.896 | Ti(2,1,3)–Ti(2,2,3) 3.122 | Ti(2,1,4)–Ti(2,2,4) 2.888 | Ti(2,1)–Ti(2,2) 2.787 |
| | | In the $[010]_{RT}$ chains | | | | |
| Ti(1,1)–Ti(1,2) 3.071 | Ti(1,1,0)–Ti(1,2,3) 3.068 | Ti(1,1,1)–Ti(1,2,2) 3.097 | Ti(1,1,2)–Ti(1,2,1) 3.104 | Ti(1,1,3)–Ti(1,2,0) 3.128 | Ti(1,1,4)–Ti(1,2,4) 3.129 | Ti(1,1)–Ti(1,2) 3.093 |
| Ti(1,2)–Ti(1,2) 3.281 | Ti(1,2,0)–Ti(1,2,3) 3.313 | Ti(1,2,1)–Ti(1,2,2) 3.277 | Ti(1,2,2)–Ti(1,2,1) 3.277 | Ti(1,2,3)–Ti(1,2,0) 3.313 | Ti(1,2,4)–Ti(1,2,4) 3.282 | Ti(1,2)–Ti(1,2) 3.391 |
| Ti(2,1)–Ti(2,2) 3.114 | Ti(2,1,0)–Ti(2,2,2) 3.204 | Ti(2,1,1)–Ti(2,2,1) 3.094 | Ti(2,1,2)–Ti(2,2,0) 3.090 | Ti(2,1,3)–Ti(2,2,4) 3.216 | Ti(2,1,4)–Ti(2,2,3) 3.026 | Ti(2,1)–Ti(2,2) 3.143 |
| Ti(2,2)–Ti(2,2) 3.239 | Ti(2,2,0)–Ti(2,2,2) 3.229 | Ti(2,2,1)–Ti(2,2,1) 3.298 | Ti(2,2,2)–Ti(2,2,0) 3.229 | Ti(2,2,3)–Ti(2,2,4) 3.269 | Ti(2,2,4)–Ti(2,2,3) 3.269 | Ti(2,2)–Ti(2,2) 3.266 |

*Note.* The standard deviations on the Ti–Ti distances are 0.001 Å at 298 and 115 K and 0.002 Å at 140 K.

$Ti_7O_{13}$ and $Ti_8O_{15}$ samples were analyzed and had a total impurity content lower than 0.1% with 65 ppm of Zr as the largest transition metal impurity. The present sample is therefore chemically closer to the sample in (*2*) than to the one in (*14*). The cell data from the three samples agree well at RT and IT. As for the LT phase, a good agreement is observed between the lattice parameters of the present sample and the corresponding ones for $(Ti_{0.9975}V_{0.0025})_4O_7$, while the LT cell data from Ref. (*2*) appear to be discrepant. The latter data show no significant change at the LT transition, a surprising observation in view of the dramatic structural change that is observed to occur. It has been shown that the incorporation of more than 0.35% of vanadium suppresses the LT transition (*15*). The cell data of Ref. (*2*) were obtained by the use of a specially prepared powder for which there was no experimental evidence that it transformed at the lower transition. It is conceivable that the powder used in Ref. (*2*) did not undergo the LT transition because of stoichiometric problems.

The variation of the lattice parameters and unit cell volume as a function of temperature for a $(Ti_{0.9975}V_{0.0025})_4O_7$ sample showed two discontinuities corresponding to IT and LT transitions, respectively (*14*). These data were obtained on the single crystal used for structural work. The present sample is not ideally pure, however the new values of the lattice parameters, reported in Table I, strongly indicate that equivalent discontinuities should exist for totally pure $Ti_4O_7$.

The 298 K (RT) and 115 K (LT) structures are essentially as described in (*2*) except that the distances and angles in the LT phase differ slightly due to cell parameter change. However, the bond valence summation (*11, 5*) supports the previous conclusion (*2*) that all the Ti valences at RT are close to 3.5 while they separate into $3^+$ and $4^+$ at LT.

TABLE IV

CELL PARAMETERS FROM REFS (*2*, *14*) IN THE PRESENT SYSTEM OF AXES

| | $Ti_4O_7$ (*2*) | | | $(Ti_{0.9975}V_{0.0025})_4O_7$ (*14*) | | |
|---|---|---|---|---|---|---|
| | 298 K | 140 K | 120 K | 298 K | 135 K | 100 K |
| $a$ (Å) | 5.593 | 5.590 | 5.591 | 5.594 | 5.594 | 5.624 |
| $b$ (Å) | 7.125 | 7.128 | 7.131 | 7.122 | 7.130 | 7.198 |
| $c$ (Å) | 20.425 | 20.380 | 20.394 | 20.419 | 20.352 | 20.253 |
| $\alpha$ (°) | 67.63 | 67.70 | 67.68 | 67.70 | 67.77 | 67.89 |
| $\beta$ (°) | 57.14 | 57.36 | 57.36 | 57.16 | 57.43 | 57.70 |
| $\gamma$ (°) | 108.73 | 108.89 | 108.89 | 108.76 | 109.02 | 109.68 |
| $V$ (Å$^3$) | 464.56 | 464.90 | 465.38 | 464.48 | 464.93 | 466.58 |

On the contrary, the 140 K structure is radically different from the one previously reported (*2*). As has been observed for $Ti_6O_{11}$, we observe here a long-range order of the Ti valences shown in Fig. 1 and a Ti–Ti bonding pattern whose distances are given in Table IV. The Ti valences are found to be alternately $3^+$ and $4^+$ in adjacent slabs parallel to $(10\bar{2})_{IT}$ which corresponds to the $(25\bar{1})$ plane of the pseudorutile lattice. At the contact between the slabs, isolated ions carry intermediate charges. This situation is different from that found in $Ti_6O_{11}$, where $Ti^{3.5+}$ ions form pairs.

In the LT phase of $Ti_4O_7$ the cation charges are ordered in such a way as to form alternate layers of $Ti^{3+}$ and $Ti^{4+}$ octahedra perpendicular to the [010] pseudorutile direction, that is parallel to the hexagonal close-packed layers of oxygen (*13*). At the LT transition, the alternate slabs of $Ti^{3+}$ and $Ti^{4+}$ octahedra, which in the IT phase are parallel to the $(25\bar{1})$ pseudorutile plane and are two-octahedra thick, swing around and become parallel to the (010) pseudorutile plane. In addition the two-octahedra thick slabs become monolayers.

The positive correlation between the change in Ti–Ti distance in the rutile-like chains and the change in ionic repulsion between the Ti ions noticed in $Ti_6O_{11}$ are seen here as well and manifest themselves by the compression of the $3^+$ slabs and the extension of the $4^+$ ones. This peculiar pattern of Ti atom displacement is in turn responsible for the above-mentioned modulation of the diffracted intensities.

Magnetic susceptibility and ESR measurements point at a single magnetic discontinuity at the higher transition (*3*) where complete pairing of $Ti^{3+}$ ions appears to occur. Comparison with previously reported structural results which indicated a somewhat disordered charge localization led to interpret the 140 K phase as a "liquid of bipolarons" (*3*, *13*) and to ascribe its conductivity to bipolaronic mobility. The present results show that the Ti valences are essentially ordered by the modulation and $Ti^{3+}$ pairing is seen. The sharpness of the superstructure diffraction peaks indicates that long-range order of the pairs exists over at least $10^3$ Å. The present results are therefore inconsistent with the hypothesis of independently mobile bipolarons. The interpretation of the conductivity in this phase should therefore be revised.

The present results are consistent with a large drop in the spin count at the higher transition, but another drop is expected at

the lower transition because the $Ti^{3+}$ pairing is seen to be incomplete at IT. Although the structural and magnetic results could be reconciled by accepting static or local dynamic disorder of the pairs in the IT phase (but not long-range dynamic disorder which would preclude the occurrence of sharp superstructure reflections), we rather suggest that an accurate spin count should be performed on a well characterized sample of pure $Ti_4O_7$ at the lower transition before interpreting the structural results in terms of the magnetic ones.

The similarity between the low-temperature behaviors of $Ti_4O_7$ and $Ti_6O_{11}$ which prompted this study is only partial at the microscopic level. Although the transition temperatures are strikingly similar and the ordering of Ti valences seems to be the driving mechanism in both cases, the $Ti_2^{7+}$ clusters which dominate the magnetic behavior of $Ti_6O_{11}$ (*12*) are not seen in $Ti_4O_7$. The pairing of $Ti^{3+}$ ions which is observed to be complete within experimental error at 115 K is apparently partial at 140 K.

It is usually observed that on cooling, phase transitions are accompanied by a loss of symmetry elements. For instance, the two transitions in $Ti_6O_{11}$ and the IT transition in $Ti_4O_7$ follow this rule, in each case the multiplicity of the superstructure increases on cooling. On the contrary the LT transition in $Ti_4O_7$ violates it as the superstructure occurs on heating.

## Acknowledgments

We thank Dr. Pierre Strobel for the single crystal used here and Dr. L. D. Calvert and Dr. C. M. Hurd for discussions and encouragements.

## References

1. A. D. Inglis, Y. Le Page, P. Strobel, and C. M. Hurd, *J. Phys. C. Solid State Phys.* **16,** 317 (1983).
2. M. Marezio, D. B. McWhan, P. D. Dernier, and J. P. Remeika, *J. Solid State Chem.* **6,** 213 (1973).
3. S. Lakkis, C. Schlenker, B. K. Chakraverty, R. Buder, and M. Marezio, *Phys. Rev. B* **14,** 1429 (1976).
4. Y. Le Page and P. Strobel, *J. Solid State Chem.* **44,** 273 (1982).
5. Y. Le Page and P. Strobel, *J. Solid State Chem.* **47,** 6 (1983).
6. Y. Le Page and P. Strobel, submitted for publication.
7. Y. Le Page and P. Strobel, *J. Solid State Chem.* **43,** 314 (1982).
8. P. M. de Wolff, T. Janssen, and A. Janner, *Acta Crystallogr. A* **37,** 625 (1981).
9. G. Germain, P. Main, and M. M. Woolfson, *Acta Crystallogr. A* **27,** 368 (1971).
10. M. Marezio, D. Tranqui, S. Lakkis, and C. Schlenker, *Phys. Rev. B* **16,** 2811 (1977).
11. W. H. Zachariasen, *J. Less-Common Metals* **62,** 1 (1978).
12. S. A. Fairhurst, A. D. Inglis, J. R. Morton, K. F. Preston, and Y. Le Page, *Chem. Phys. Lett.* **95,** 444 (1983).
13. C. Schlenker and M. Marezio, *Philos. Mag. B* **42,** 453 (1980).
14. J. L. Hodeau and M. Marezio, *J. Solid State Chem.* **29,** 47 (1979).
15. S. Ahmed, C. Schlenker, and R. Buder, *J. Magn. Mater.* **7,** 338 (1978).